Chapter 26
High-Resolution fMRI

Essa Yacoub, Amir Shmuel and Noam Harel

Feasibility

A fundamental understanding of how the human brain works requires noninvasive neuroimaging methods with sufficient spatial specificity and resolution to probe neuronal architectures such as cortical columns or interlaminar connections. Of all neuroimaging modalities, functional magnetic resonance imaging (fMRI) has shown the promise of achieving such goals. Since its introduction (Bandettini et al. 1992; Kwong et al. 1992; Ogawa et al. 1992), fMRI has evolved to become the premiere tool for mapping brain function in humans. Early fMRI studies were conducted on research magnets operating at 1.5 T, the highest field strength available for clinical MRI instruments at the time, and, in the case of the work conducted at the University of Minnesota (Ogawa et al. 1992), at 4 T which represented the highest field available for human studies at the time, however, propelled largely by fMRI, human imaging has been pushed to magnets operating regularly at 7 T at the present, and with fields as high as 10.5 and 11.7 T in the planning (e.g., Uğurbil 2012, 2014; Uğurbil et al. 2003).

The possible advantages of high magnetic fields for fMRI were first realized in the early modeling studies (Ogawa et al. 1993) (also see Uğurbil et al. (2009) and references therein) of the blood oxygenation level-dependent (BOLD) effect (Ogawa et al 1990) and was clearly demonstrated several years ago with the first human fMRI experiment at 7 T (Yacoub et al. 2001). Under appropriate experimental conditions, increasing magnetic fields can result in supralinear gains in the contrast-to-noise ratio (CNR) for functional maps due to field-dependent gains in

E. Yacoub (✉) · A. Shmuel · N. Harel
Center for MR Research, University of Minnesota, Minneapolis, MN, USA
e-mail: yaco0006@umn.edu

A. Shmuel
Montreal Neurological Institute and Hospital, McGill University, Montreal, QC, Canada

K. Uludağ et al. (eds.), *fMRI: From Nuclear Spins to Brain Functions,*
Biological Magnetic Resonance 30, DOI 10.1007/978-1-4899-7591-1_26

the signal-to-noise ratio (SNR; Vaughan et al. 2001) and the susceptibility contrast of the BOLD effect. These gains impart numerous advantages to the study of brain function, including the acquisition of higher-resolution functional images. However, because fMRI relies on the hemodynamic response to map brain function, the ability to obtain high-resolution images *alone* does not guarantee increases in the effective resolution of the functional maps.

There are in principle several fMRI techniques (with different vascular sensitivities) that could be used for functional mapping at low or high magnetic fields. Because of its ease of implementation and its relatively high CNR, gradient-echo (GE)-based, T_2*-weighted fMRI technique is almost always employed in contemporary studies of human cognition. At lower fields (≤3 T), where the majority of fMRI studies are still conducted, the spatial specificity (Engel et al. 1997; Shmuel et al. 2007; Parkes et al. 2005; Chaimow et al. 2015) and sensitivity of conventional gradient echo (GE) fMRI is sufficient for the supra-millimeter resolution neuroscience questions that are typically pursued at these low field strengths. There are only limited advantages to running such low-resolution fMRI studies at high magnetic fields because of the field-dependent increases in the contribution of physiological process to temporal noise in an fMRI time series (Hyde et al. 2001; Kruger and Glover 2001; Triantafyllou et al. 2005). At resolutions high enough to pursue functional imaging studies, for example, at the level of cortical columns and laminae, the temporal noise of an fMRI series becomes dominated by thermal noise (i.e., the intrinsic SNR of the images in the time series); at these resolutions, however, functional mapping fails at low magnetic fields primarily because the intrinsic SNR is insufficient. In contrast, at high fields, the gains in intrinsic SNR together with field-dependent elevation in functional mapping signals, particularly from the microvasculature, can be translated into higher spatial resolution, permitting the investigation of more elementary functional computations. Therefore, the high field gains in fMRI are of most benefit if they are traded in for spatial resolution or used for applications, which are SNR starved at low fields.

It can be argued that such high-resolution, column-level studies are dispensable since increased sophistication of multi-voxel pattern analysis (Haushofer et al. 2008; Haxby et al. 2001; Haynes and Rees 2005; Kamitani and Tong 2005) have demonstrated that low-resolution fMRI data at low fields can reveal details about the information encoded by different neural responses in a given cortical area. However, the underlying spatial organization of the neural architecture cannot be resolved with these methods. Moreover, fMRI-based decoding does not rely on information at the high spatial frequency that defines the spatial organization of orientation or ocular dominance maps (Chaimow et al. 2011). Instead, it relies on lower spatial frequencies of the organization (Shmuel et al. 2010; Swisher et al. 2010) and also on selective signals from macroscopic blood vessels (Shmuel et al. 2010). Further, the decoding of the high spatial frequency cortical information with low-resolution fMRI relies on a large cortical area being devoted to a particular type of information (i.e., orientation in visual cortex), which is certainly not always the case. As such, high-resolution (and thus high-field) fMRI data in the general case are still essential in the resolution and interpretation of neuronal populations.

The utility of higher spatial resolutions in fMRI at any field strength can be limited not by the resolution attained in the imaging sequence, but spatial limitations imposed by the vascular contributions of the functional mapping signals (Boxerman et al. 1995; Duyn et al. 1994; Frahm et al. 1994; Gati et al. 1997; Lai et al. 1993; Uludağ et al. 2009). Therefore, it is pertinent to understand the resolution limits of the BOLD signal in terms of specificity (i.e., fidelity to the spatial location displaying altered neuronal activity) and sensitivity. Further, since there are added technical limitations with high-field and high-resolution acquisitions, it is important to investigate how these can be alleviated with software and hardware developments to provide a more general tool for neuroscientists. To date, the limitations of high magnetic fields (i.e., short T_2*, increased physiological noise, susceptibility effects, B_1 inhomogeneities, power deposition (synthetic aperture radar, SAR), etc.) have restricted the impressive gains in spatial resolution at high fields to sections of the cortex examined with a reduced field of view (FOV), severely limiting its general application. Further, despite the extraordinary successes of spin-echo (SE) BOLD signal sequences at high fields (Yacoub et al. 2007, 2008), this approach is even more difficult to implement and apply because it is more hampered by B_1 inhomogeneities and SAR confounds. However, with the advent of parallel imaging (PI; Pruessmann et al. 1999; Sodickson et al. 1999), introduction of slice accelerated multiband techniques for fMRI to alleviate the long volumetric repetition time (TR) associated with high resolution (Moeller et al. 2008, 2010) and continued improvements in gradient and radio frequency (RF) hardware, the restrictions of high fields and thus high-resolution fMRI continue to be alleviated, diminishing the need for trade-offs between spatial specificity, resolution, or volume coverage.

Spatial Specificity of BOLD Signals

The BOLD signal measures the hemodynamic response to neural activity by exploiting the magnetic properties of blood water. BOLD fMRI is sensitive to changes in cerebral metabolic rate of oxygen ($CMRO_2$), cerebral brain flow (CBF), or cerebral brain volume (CBV), all of which alter the relative amount of deoxyhemoglobin, and thus the local magnetic field in the brain. In addition, the fMRI signal is directly sensitive to changes in CBV, which alters the amount of protons in the extra- and intravascular spaces (Uludağ et al. 2009). GE and SE BOLD fMRI at low fields are subject to a dominating (similar) intravascular blood effect that cannot be suppressed by longer echo times because of the long blood T_2 at these fields. Since the blood T_2 is extremely short at high fields, the intravascular effect is diminished for both SE and GE at high fields (Duong et al 2003), the extravascular effect becomes dominant, and, ultimately, we are left with a BOLD signal that reflects extravascular effects around large and small vessels for GE and primarily small vessels for SE, since tissue signal around large vessels is refocused. While the tissue dominated SE-BOLD signal has less total (small and large vessel) CNR compared to GE at 7 T, the tissue CNR is sufficient in SE BOLD to investigate submillimeter functional organizations. It should also be noted that, provided large vessel effects can be explicitly avoided or suppressed, which is not always feasible in the human, GE-BOLD signals

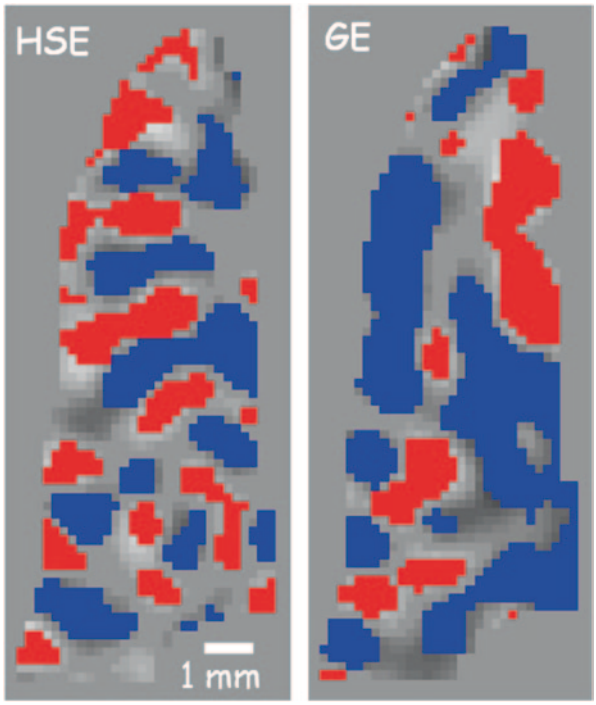

Fig. 26.1 ODC maps from a flat gray matter region along the calcarine sulcus from the same subject on several different days. On the *left* is the overlap of two different scan days using SE at 7 T, while on the *right* is the overlap of two different scans using GE. *Red* or *blue* pixels indicate a voxel's preference to right or left eye stimulation. The expected spatial pattern is an alternating preference (1 mm width, 2 mm cycle) to right or left eye running along the sulcus. The SE map retains this pattern throughout the region, while the GE map is interrupted by extravascular changes around large vessels somewhere near the region of interest. *HSE* Hahn spin-echo, *GE* gradient echo (Taken from Fig. 5 in Yacoub et al. (2007))

can and have been used to map columnar organizations (Cheng et al. 2001; Menon et al. 1997; Moon et al. 2007; Yacoub et al. 2007). Figure 26.1 demonstrates this by showing the mapping of ocular dominance columns (ODCs) in humans at 7 T using either GE- or SE-based BOLD contrast. The cyclical pattern of the ODCs, alternating between right eye preference (red) and left eye preference (blue) every ~1 mm is resolved uninterruptedly with SE contrast, while the GE map is hampered by nonspecific vascular effects at some but not all locations, preventing the uninterrupted visualization of the columns. Thus, unlike low fields, where GE fMRI is almost always the best option, at high fields the best approach is less obvious, because there are significant spatial and temporal trade-offs (i.e., efficiency, volume coverage, specificity, etc.) between GE and SE BOLD. Although the advantages of SE BOLD at high fields was demonstrated for high-resolution fMRI applications in the limited volume case, expanded imaging volumes (more readily achievable with GE contrast) would allow for identification and avoidance of vessels, expanded coverage of activated areas, and improved anatomical registration and motion correction—making GE-BOLD also an attractive option.

Reducing Acquisition for High-Resolution Images

Acquiring images of part or the entire brain can be undesirably long for imaging of brain function in humans. With conventional GE techniques, such as fast low angle

shot (FLASH; Haase et al. 1986), it can take tens of seconds and even minutes to acquire a volume, depending on resolution and FOV. In order to obtain maximum acquisition speeds, ultrafast imaging techniques, such as echo planar imaging (EPI; Mansfield 1977) (rectilinear) or spiral acquisitions (Glover 1997; Meyer et al. 1992; Noll et al. 1995), are commonly used for fMRI. Even using these fast acquisition schemes, the data readout time to sample *k*-space for a single image can be long (compared to the T_2^*), especially for high-resolution acquisitions. This leads to signal loss, increased geometric distortions and overall poorer image quality.

At lower fields, the T_2^* is longer and, as a result, there is more time for *k*-space sampling; however, high spatial resolution cannot (generally) be achieved because of overall SNR limitations. At high fields, high spatial resolution applications based on EPI or spiral readouts have typically employed multi-shot segmented (vs. single shot) *k*-space coverage to reduce the amount of data acquired after a single excitation, thus allowing for shorter echo times and readout trains to accommodate the short T_2^*. For example, in a high-resolution human study, Cheng et al. (2001) used 32 image segmentations (volume TR of ~10 s), while a high-resolution monkey study (Goense and Logothetis 2006) also employed large amounts of segmentation. Recent work investigating ODCs (Yacoub et al. 2007) and orientation columns (Yacoub et al. 2008) in the human used a significantly reduced number of image segments.

Image segmentation comes at the expense of temporal resolution and segmentation errors associated with physiological fluctuations, subject motion, as well as instrumentation inaccuracies. For GE imaging, ultrashort intersegment (<1 s) TRs can be used since there is enough SNR and SAR is not limiting, making large amounts of segmentation feasible, although suboptimal. For SE imaging in humans at 7 T, due to SAR and SNR considerations, such short intersegment TRs are not possible making fMRI acquisitions with more than a few segments, nearly impossible. In either case, since the statistical significance of functional signal changes can be dictated by temporal instabilities in the fMRI time series and not thermal noise (i.e., noise that determines the SNR of a single image), the use of image segmentation to increase SNR or reduce the readout time, at the expense of longer total acquisition times is not ideal.

The need for segmentation can be ameliorated or even eliminated using PI techniques (Pruessmann et al. 1999; Sodickson et al. 1999), which reduce the number of acquired phase encode lines by a factor *R,* resulting in a proportional decrease in the total readout time, without a sacrifice in the imaged FOV; the aliased signals are then unfolded using coil sensitivity profiles of the receiver array coil. This does, however, come at the expense of a reduced image SNR due to *R*-fold fewer data points collected per image due to undersampling and the imperfections introduced in the image reconstruction based on coil sensitivity profiles, which appears as a spatially nonuniform noise and is characterized by a parameter referred to as the geometry- (or *g*-) factor. The net SNR loss is then given. However, the loss in image SNR due to PI does not necessarily translate into a corresponding reduction in functional CNR. This is true when the functional CNR is dominated by processes, such as physiologically induced signal fluctuations, instead of thermal noise. This has been amply demonstrated in previous studies (de Zwart et al. 2002; Moeller

et al. 2006). In contrast, an additional gain in functional CNR can be attained despite the reduction of image SNR from PI over segmented approaches; this gain arises because segmented acquisition (as opposed to single shot) amplify the deleterious contributions by physiological processes, such as respiration and heartbeat, into the temporal fluctuations in the fMRI time series. Just like FLASH images were shown to be prone to higher temporal instabilities compared to single-shot EPI (Hu and Kim 1994; Hu et al. 1995), segmented EPI is more prone than single-shot EPI. Furthermore, this problem gets worse with increasing field strength, because physiologically induced fluctuations increase (Hyde et al. 2001; Kruger and Glover 2001; Triantafyllou et al. 2005). This was demonstrated in recent work (Moeller et al. 2006) where fMRI images acquired with a four segment EPI acquisition were compared to reconstructing the data with only one segment (1/4 of the data), and unaliasing the resulting images with SENSE. This resulted in virtually identical functional CNR, despite the $g(R)^{1/2}$-fold intrinsic loss in SNR. Furthermore, when four times as many images were acquired using PI over the same acquisition time, 30–60 % improvements in functional statistical significance were observed.

In addition to PI, another strategy to reduce the number of segments (or readout time) needed to obtain higher spatial resolutions is to reduce the FOV without aliasing, and thus the number of phase encoding (PE) steps needed to achieve the same resolution. To reduce the imaging FOV without signal folding, one can use outer volume suppression (OVS; Pfeuffer et al. 2002; Schafer et al. 2007), smaller coils that "see" a smaller amount of the brain, or selectively excite only the area of interest (inner volume, IV) excitation; Duong et al. 2002; Feinberg et al. 1985; Yacoub et al. 2003; Yang et al. 1997). These options (along with PI) may be used in conjunction with each other for further optimization. OVS techniques may be implemented; however, because of the magnetization transfer effect, they result in SNR losses of up to 30 % (Pfeuffer et al. 2002) and are SAR limited, especially at high fields. We previously used and developed an IV approach for reduced FOV imaging for SE (Duong et al. 2002; Yacoub et al. 2003) acquisitions. In this sequence, a slice selective 90° excitation pulse is followed by a slab-selective (along the PE direction) refocusing pulse. This permits a reduction of the phase FOV (and thus the number of PE lines), and ultimately fewer segments and a shorter TR. However, due to IV orthogonal RF pulses cross-irradiating images, it has not been possible to achieve multi-slice 2D IV imaging. 3D IV approaches have been proposed and used (Feinberg et al. 2008; Feinberg and Oshio 1991), allowing for much larger volume coverage. Figure 26.2 shows an example of a reduced FOV single-shot EPI image using 3D gradient and spin echo (GRASE; Feinberg and Oshio 1991) with IV selection. The use of surface coils is often ideal when only a portion of the brain needs to be imaged, allowing for a more open (fMRI-friendly) coil design, rather than the typical total encompassing head coil, which leaves little access to the subject. Such a coil design does not see the entire brain, permitting the reduction of the FOV without signal folding—and thus the ability to obtain high-resolution images efficiently, albeit over limited volumes. For very high spatial resolution applications (i.e., 0.5 mm in plane) in humans at 7 T, despite using both a surface coil and

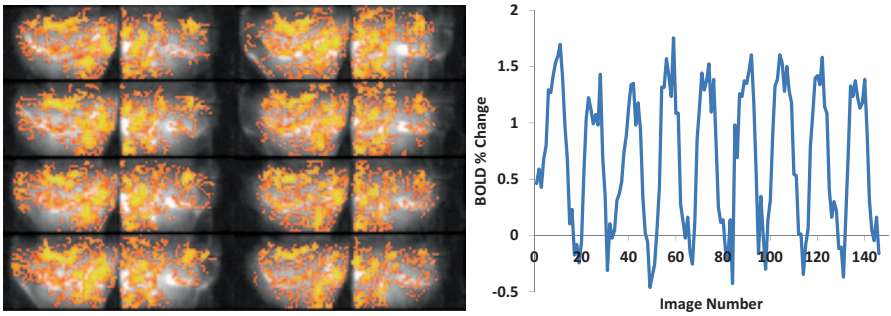

Fig. 26.2 Example of high-resolution fMRI with a coronal slice prescription and 0.7 mm isotropic 3D GRASE acquisitions. Shown is a representative fMRI activation map, overlaid on the T_2^* weighted 3D GRASE images, along with the corresponding time course. *BOLD* blood oxygenation level-dependent

IV excitation, image segmentation was still needed, although greatly reduced (3–4 segments) over full FOV acquisitions (12–16 segments).

Ultimately, high-resolution BOLD images (at high fields) are limited by readout time durations, resulting in limited volume acquisitions and increased segmentation, which in turn results in increased temporal fluctuations and the loss of temporal dynamics as well as functional sensitivity in fMRI. This has significantly hampered the ability of high-field fMRI to map high-resolution structures and/or conduct large volume or whole brain studies in humans with higher-spatial resolutions.

Volume Coverage in High Resolution fMRI

Limited volume coverage can be detrimental to the success of high-resolution fMRI in humans. First, one needs to search for an optimal slice or region of interest, preferably with minimal curvature in the gray matter. Otherwise, it becomes difficult to understand and/or characterize the functional organizations as the structures and patterns cannot be easily discerned (Cheng et al. 2001; Yacoub et al. 2007, 2008). This ultimately limits the general application of these methods to prescreened subjects, which requires additional scanning sessions, and limits the pool of subjects that can be studied. Second, with this limited imaging volume, slight motion of the subject and/or mis-positioning of the slice will result in a total loss of any useful functional information as the imaged slice may move into white matter areas or regions outside the cortical area that would not be expected to show such functional patterns. Third, motion compensation, which can be desirable for these high-resolution images in humans, is extremely limited because once the slice has moved out of the region of interest (ROI) the acquired images are no longer relevant to the functional patterns being mapped. This further limits the subject pool to well-trained subjects who have

the ability to be still for long periods of time. Therefore, the ability to image highly specific functional signals with reduced acquisition times and over a 3D or larger volume, having millimeter or submillimeter in plane resolutions, will significantly facilitate probing the human brain at the level of detail needed for a better understanding of the functional organization of cerebral cortex.

RF Coils for High-Resolution fMRI

Many factors affect the choice of RF head coil for an experiment. At standard field strengths, head coils tend to be receive-only designs, whereas at 7 T, body RF coils are not typically used and thus localized transmit and receive head coil designs are needed. Although such RF transmit approaches, along with multichannel transmit, can be optimal for 7 T applications, they can be problematic for fMRI experiments where a sufficient amount of space is needed for visual presentation. More and more whole-brain coils are being designed for 7 T that permit a larger FOV, keeping elements away from the eyes, while not impinging on the ability to achieve efficient whole-brain coverage. To make RF coil design even more challenging, if high-performing (desirable) head gradients are used, the space inside the bore decreases significantly. As such, for visual fMRI studies, open- (half-volume) design surface coils (or arrays) are often used, especially for ultrahigh-resolution studies of visual cortex.

More obvious factors in coil selection and experiment design are related to sensitivity, power requirements, PI performance, and uniformity of coverage. Using a surface coil for data acquisition, or a local array of surface coils, is a common way of increasing SNR for high-resolution experiments. Obviously, this is an option only for applications in which extended brain coverage is not needed and the cortical ROI is readily accessible using a surface coil—generally, primary cortical sensory and motor areas. The nonuniform sensitivity profiles of surface coils present a challenge for applications requiring uniform contrast between gray and white matters, but it has recently been shown that if a T_1-weighted volume is normalized by a simultaneously acquired proton density-weighted volume (Van de Moortele et al. 2009), cortical surface segmentation is possible even on partial-brain anatomies acquired with surface coils (Olman et al. 2010). Finally, surface coils with an open design are also much more accommodating to the use of bite bars to restrict subject motion, which can be critical to the success of high-resolution fMRI applications (Yacoub et al. 2007, 2008).

Since there are many factors in determining the ideal RF coil, application-specific decisions are typically made. Clearly, where large volume coverage is warranted, whole brain coils are needed, while a need for accessibility to the subject requires more open-coil designs which can be optimized for the cortical region of interest, at the expense of volume coverage. However, as RF coil technology and design continue to evolve, it is conceivable that a single design may eventually be optimal for a vast majority of fMRI studies.

Pulse Sequence Options

As mentioned, the overwhelming majority of human fMRI studies rely on the susceptibility-based BOLD effect, mainly because of its high CNR. However, to achieve BOLD contrast, a plethora of MR pulse sequences have been proposed. The choice of pulse sequence is weighted strongly by the demands of the neuroscience question being asked. For example, while a better understanding of the hemodynamic response function (i.e., event-related fMRI) warrants higher temporal resolutions, the mapping of intrinsic functional architectures of neuronal organization requires high spatial resolution. Further, it is difficult to acquire high spatial resolution data with high temporal resolution, and the reduced power of event-related designs makes these difficult to execute at very high resolution. Applications such as resting-state fMRI would ideally want high spatial and temporal resolution, as well as large-volume or whole-brain coverage. To make things even more complicated, the spatial resolution requirements of the neuroscience question (i.e., 2–3 mm vs. 1 mm or less) are also highly relevant when choosing acquisition parameters or pulse sequences, as trade-offs would be made between CNRs and spatial specificity.

Alternatives to EPI

To date, nearly all fMRI studies at both low and high fields utilize 2D or 3D single- (or multi-) shot EPI (Mansfield 1977; Mansfield et al. 1994) or spiral-based acquisitions (Glover 1997; Lee et al. 1995; Noll et al. 1995; Yang et al. 1996) due to the efficiency of the sequence, which is paramount for fMRI studies. For example, FLASH imaging (Haase et al. 1986), which has been successfully implemented, requires extremely long acquisition times (30 s–1 min) and are not practical for most human fMRI studies (Frahm et al. 1992, 1993; Koopmans et al. 2010). Radial methods (Silva et al. 1998), which are less sensitive to physiological noise and motion, over-sample the center of *k*-space, particularly k_0, making it less efficient in terms of *k*-space coverage per sequence time. Cases can be made to utilize non-EPI-based acquisitions for some applications which require reduced distortions, motion artifacts, or susceptibility effects. However, the vast majority of fMRI studies cannot afford the penalty in efficiency, especially since there are numerous ways to mitigate artifacts in EPI.

2D Versus 3D Approaches

Most fMRI studies typically employ single-shot 2D EPI acquisitions because the acquisition time for a single slice as well as for an entire volume is extremely fast (on the order of millisecond for a slice and 2–3 s for a volume). While 3D sequences have the advantage of higher SNRs (due to the 3D fast Fourier transform, FFT), the acquisition time for a given slice is convolved over the volume acquisition time

(2–3 s), making the acquisition highly sensitive to motion and physiological noise. Such a long volume acquisition time is required as the 3D acquisition is usually segmented to prevent long readouts. This is similar to the long slice TRs and resulting physiological noise present in segmented 2D EPI acquisitions. Further, employing 3D acquisitions can result in blurring as well as aliasing along the slice direction. Historically, this has resulted in the use of 2D techniques for most applications, and 3D approaches when a large number of slices are required, when temporal resolution is not critical, or when SNR is limiting in 2D acquisitions.

However, both 2D and 3D acquisitions can capitalize on accelerated acquisitions using phase encode reductions. Since 3D utilizes two phase-encoding directions, accelerations along two dimensions can be achieved, reducing even more the acquisition times and allowing for much more efficient 3D acquisitions. Poser et al. (2010) showed that with the ability to accelerate along the slice direction, the 3D acquisition time was reduced to levels faster than what can be achieved with 2D imaging, resulting in an overall improved performance of 3D functional images over 2D. This study, however, did not utilize a recently implemented slice-acceleration technique (multibanded EPI) for 2D acquisitions, which allows for up to a fourfold faster volume TR without losses from data undersampling (Larkman et al. 2001; Moeller et al. 2010), as is present in 2D accelerations of 3D acquisitions. 3D Principles of Echo-Shifting with a Train of Observations (PRESTO) SENSE (Golay et al. 2000; Klarhofer et al. 2003; Liu et al. 1993; Neggers et al. 2008; a multi-shot 3D EPI technique) has also been proposed to significantly reduce the acquisition using the dead (TE preparation) time between the RF pulse and the subsequent readout to apply the next excitation pulse, and then separating the readouts by echo shifting. The utility of this technique depends on the required TE and at 7 T, due to the shorter TEs used, there is not enough (dead) time to acquire the shifted echoes from the previous excitation.

Ultimately, the choice between 3D and 2D acquisitions is determined by (1) whether or not the 3D acquisition time can be reduced enough so that physiological noise issues do not impede on the 3D functional sensitivity, and (2) whether or not accelerated 2D acquisitions have sufficient static SNRs. Further, for ultrahigh-resolution applications, the use of isotropic resolutions requires ultrathin slices which can be problematic for 2D acquisitions because of slice profile issues in addition to the low SNR of the high-resolution images. To date, although there are more and more papers establishing the superiority of 3D techniques for many applications, continued improvement of the efficiency and quality of 2D techniques (resulting from advances in MR technology such as gradient performance, RF coils, pulse sequence design, etc.) have allowed 2D techniques to remain the most attractive to neuroscientists—even for high-resolution applications.

Spin Echo Based Contrast

High-resolution neuroscience questions can and are being asked at high fields. Therefore, the presence of highly specific BOLD signals becomes a concern when

deciding on a pulse sequence. So, at the expense of reduced contrast to noise, T_2-weighted approaches can and have been employed to address these high-resolution questions (Yacoub et al. 2007, 2008), albeit with a different set of limitations compared to GE acquisitions. First, extremely fast TRs are not typically employed, certainly not for high spatial resolution images, due to the insufficient SNR. The low SNR is likely the result of inhomogeneous RF fields which reduce flip angles and subsequent image SNR. This problem is significantly magnified in SE images over GE images because of the need for a 180° refocusing pulse in SE acquisitions. Further, at 7 T, where SE acquisitions are typically employed because of increased sensitivity and specificity of BOLD images, faster or even efficient acquisitions are difficult to achieve because of SAR.

Given all of these practical constraints for the implementation of SE BOLD techniques, the sequence options are more limited. Although sequences such as steady-state free precession (SSFP; Miller and Jezzard 2008), half-Fourier-acquired single-shot turbo spin echo (HASTE; Poser and Norris 2007; Ye et al. 2010) (or turbo spin echo, TSE/fast spin echo, FSE) have all been proposed for T_2-weighted BOLD, none of them have achieved the necessary combination of efficiency, spatial resolution, functional contrast and specificity to be viable for ultrahigh-resolution applications, which are the main reason for using T_2-weighted BOLD in the first place. To date, only 2D SE-EPI has demonstrated a neuroscience utility as well as an advantage over conventional GE-EPI. In this application, albeit using a reduced-FOV approach that was necessary to achieve efficient high-resolution T_2-weighted images, 2D EPI was shown to be a better alternative than GE EPI, allowing the uninterrupted mapping of ocular dominance (Yacoub et al. 2007) and orientation columns (Yacoub et al. 2008) in humans. In addition, the spatial specificity obtained by SE contrast is better than that of GE contrast (Chaimow et al., 2015). Under development are 3D variations of reduced FOV 2D-EPI (i.e., 3D GRASE; Yacoub et al. 2009), which provide a means to efficiently extend the volume coverage of 2D EPI, while maintaining functional specificity (see Fig. 26.2).

Human Subjects and Scan Planning

Head Movements

As described above, current methods of fMRI at the spatial resolution of cortical columns and lamina offer limited static signal to noise, dynamic signal to noise, and CNRs. In addition, cortical columns are organized at high spatial frequency parallel to the cortical manifold (e.g., ~1 cycle/2 mm for ocular dominance and orientation columns). To be able to capture these organizations in spite of the limited signal and contrast to noise, it is essential to image for as long as possible while minimizing movements to a small fraction of a millimeter for the entire imaging duration. Procedures that can support the achievement of these conditions are described below.

In order to minimize movements for a long duration, the subject needs to be comfortable. Appropriate support under the body, and especially below the head, will prevent pain due to pressure caused by laying on the hardened patient bed or the surface of the RF coil, respectively. Tempur-pedic foam has been found to be efficient for both purposes. In supporting the head for imaging the visual cortex, one may face a trade-off between comfort and SNR: The thicker the foam used, the more comfortable the subject is, but also the more distant the brain is from the surface coils typically used in these applications. In addition, one needs to consider a minimal interval of several days between successive scan sessions, in order to allow recovery of the subject from these pressure effects.

While eliminating head-movements is essential, it is also important, especially at ultrahigh fields, to instruct subjects to keep their body and limbs still for the duration of the scan. Movements of these parts of the body may introduce small, unintended movements of the head. In addition, they are prone to modifying the magnetic flux near the head, thus requiring additional B_0 shimming.

It is commonly assumed that subjects may relax and move in between individual scans within a session. This may be reasonable with applications at low resolutions or when large volumes of the brain are imaged and therefore alignment of volumes by post-processing ("motion correction") is efficient. In contrast, any movement, either within a scan or between scans, is prone to hamper efforts of imaging at the resolution of columns and laminae. To start with, movements cause the mixture of signals from domains of different functional specificity. In addition, they can be detrimental to optimized local volume shimming done at the beginning of the session.

The smaller the imaged volume, the more problematic movements are. In the extreme case of imaging one slice (Shmuel et al. 2007; Yacoub et al. 2007), it is helpful to monitor the position of the head by taking anatomical images oriented perpendicularly to the imaged functional slice during the time between functional scans. Any substantial movement of the head along the axis orthogonal to the imaged functional slice requires immediate repositioning. Otherwise, the structure which is imaged, typically a flat gray matter region, will remain outside of the FOV or will be imaged with substantial partial-volume effects.

The small imaged volume and relatively low SNR make also the use of post-processing motion correction difficult. Motion correction algorithms seek a "repositioning" of any volume such that its repositioned coordinates and 3D angle will make it as similar as possible to one reference volume. Small imaged volumes and low SNR make the volume-to-volume search of the optimal repositioning unstable. Therefore, motion correction should be used cautiously, and in some cases it has already proven to be more harmful than useful (Cheng et al. 2001). Depending on the specific question and ROI, it may be useful to discard noisy data in regions that are not of interest prior to applying motion correction. In addition, in order to not reduce the effective spatial resolution of the images, it is advised to pursue interpolation associated with repositioning in conjunction with motion correction only once. For example, motion correction may be applied first within single scans, then between scans in a day, and then possibly between days. To minimize reduction in high spatial frequencies, one can multiply the matrices describing the translation

and rotation parameters of each volume with the reference within the scan by the matrix describing these parameters of the specific scan relative to the reference scan, and by the matrix describing these parameters of the specific day relative to the reference day. The result of this multiplication can be applied to the specific volume, so that interpolation is performed once, rather than three times.

When imaging at submillimeter resolutions, the use of devices that limit the subject's movements and guide him in trying to stay still is a necessity. For this, the use of bite bars can be extremely helpful. Bite bars are molded in a subject specific manner, so that they fit the subject's teeth tightly. Typically, subjects find it easier to comply with bite bars that cover approximately 2/3 of the teeth while avoiding the deeper portions of the mouth, compared to bite bars that cover all of the teeth. Bite bars do not lock the subject's head in position (i.e., subjects can move with bite bars). Therefore, bite bars should be considered as reference devices that guide the subjects in their efforts to not move. In this context, shortening the bite bars to 2/3 of their full potential dimensions encourages compliance, while not reducing performance.

ROI Selection, SNR, and Subject Positioning

When pursuing a high-resolution imaging session, every minute is valuable. The duration throughout which the subject can stay still in the magnet with a bite bar is limited. It is therefore important to plan the ROI localization in advance. According to the neuroscientifc question and the MRI methods used, planning can include, for example, selection of a flat gray matter region when one or a few MRI slices are scanned, or fMRI at low resolution with a paradigm relevant to the high-resolution study, etc.

As described above, high-resolution fMRI is currently pursued with limited SNR. It is therefore essential to fully maximize the available SNR. Since surface coils or a combination of surface coils are commonly used, it is important that the ROI is well localized within the volume of peak SNR of the RF transmit and receive coils. When imaging a relatively small volume, it is helpful to select the ROI as close as possible to the surface coil (within the limits allowed by the neuroscientific question) in order to maximize SNR. Since bite bars are important factors in head positioning, it is beneficial to keep track and gradually improve the subject-specific bite bar settings (position and orientation relative to the coil) with which the subject's specific ROI overlaps with the peak SNR volume produced by the RF coil. Yet another situation which requires careful planning, ROI selection, and keeping track of positioning parameters, is that of multiple sessions in which the same ROI is imaged, for the purpose of averaging, verifying reproducibility, or studying neuroplasticity. Parameters of subject positioning should be precisely reproduced, and ROI selection should be carefully planned and reproduced based on anatomical landmarks.

Finally, it is difficult to stay still for a long duration while biting a bite bar and performing a cognitive task in a closed, noisy environment. Rather than scanning

naive volunteers, it is more productive to pursue several sessions with subjects found to be able to perform well in initial, low-resolutions studies. Of course, special subject-specific features of anatomy need to be considered, such as flat gray matter within the ROI (Cheng et al. 2001; Shmuel et al. 2007; Yacoub et al. 2007), when only a few slices can be imaged.

Paradigms and Validation

Number of Conditions, and the Sequence of Stimuli Presentation

In planning a high-resolution fMRI study, one needs to consider the paradigm carefully. The main issues to consider are the number of conditions and the sequence of presentation of stimuli: event related, block paradigm, or a phase-encoding paradigm.

Due to limited static and dynamic SNR, the number of conditions in a paradigm associated with a single session needs to be minimized. Assuming independent dynamic fMRI signal changes due to resting-state and noise (an assumption which is of the "best case scenario"), one needs to acquire the square of a number volumes in order to reduce the noise in a factor equal to that number. Therefore, especially at high resolution with inherently low SNR, the number of conditions needs to be minimized. One approach that may be considered is using a small number of conditions first for establishing reproducibility (e.g., vertical and horizontal gratings), then increasing the number of conditions (e.g.,to 8 gratings spaced evenly in the orientation space).

SNR and CNR considerations also make block paradigms preferable over event-related paradigms. In event-related paradigms, imaging time is wasted on the overhead of the increase and decrease of signal from baseline (or close to baseline) to peak response. This overhead is relatively reduced in block paradigms. The same type of overhead is virtually eliminated when using PE paradigms (Engel et al. 1994; Kalatsky and Stryker 2003; Yacoub et al. 2008). However, PE paradigms require a cyclic organization of the stimuli in the stimulus space (e.g., orientation of 0–180° or direction of motion of 0–360°), otherwise they become similar, in principle, to block paradigms.

Validating Findings in High-Resolution fMRI Studies

The methodological difficulties in pursuing fMRI studies at high-resolution make exhaustive validation of the findings imperative. First and foremost, reproducibility within a session and/or across sessions should be verified. Whereas pursuing reproducibility across sessions is difficult, it is feasible (Yacoub et al. 2007). Moreover,

repeated imaging across two or more sessions enables averaging across multiple datasets, which may reveal the findings in a clearer manner and allow more powerful statistical testing. Reproducibility of findings across subjects is helpful too. Lastly, similarity of the findings to independently obtained data from humans or animal models is a strong indication that the findings are valid, the methods are robust, and therefore can be used further to explore unknown territories. For example, using SE fMRI, Yacoub et al. (2007) demonstrated (see Fig. 26.1) (1) reproducible maps of ODCs across multiple sessions in single subjects, (2) anisotropy of the columns, with the major axis of anisotropy orthogonal to the anatomically expected curve of the V1/V2 border, similar to what was previously shown in monkeys (Ts'o et al. 1990), and (3) spatial frequency (~1 cycle/2 mm) of the organization orthogonal to the axis of anisotropy that matched the findings in a previous postmortem study in humans (Horton and Hedley-Whyte 1984). This validation made it clear that the SE BOLD imaging method is robust, and paved the way for using it in investigating less known territories, such as orientation maps in humans (Yacoub et al. 2008).

Applications of High Resolution fMRI

FMRI has indeed revolutionized the field of human brain research as it has allowed for noninvasive mapping of the spatial architecture of brain function at the most finest of scales. As described above, recent advances in fMRI have led to enhanced sensitivity and spatial accuracy of the measured signals, indicating the possibility of detecting smaller and smaller neuronal ensembles that constitute fundamental computational units in the brain, such as cortical columns and lamina. In the following section, we summarize the recent applications of high-resolution fMRI studies, which aimed at resolving columnar- and laminar-level functional units in the human cerebral cortex.

Cortical Columns

A fundamental property of the cerebral cortex is the spatial localization of function. Within a defined cortical region, neurons sharing similar functional properties are often clustered together spanning from the pial surface to the white matter, thus forming a column-like functional unit. Initially, Mountcastle (1957) described the columnar organization of the somatic sensory cortex, which was followed by the work of Hubel and Wiesel (1962, 1963), who mapped the columnar organization of the visual cortex. This functional parcellation extends in the millimeter to submillimeter domain. In visual cortex, preference to right or left eye (ocular dominance), direction of motion (Shmuel and Grinvald 1996; Weliky et al. 1996), spatial frequency (Issa et al. 2000), and orientation (Blasdel and Salama 1986; Bonhoeffer and Grinvald 1991; Hubel and Wiesel 1963, 1977) have all been characterized

in animals using both classical electrophysiological as well as imaging based on optical methods. In humans, the first example of such functional domains to be identified was ODCs that were observed using anatomical staining techniques in the postmortem human brain (Horton and Hedley-Whyte 1984). ODCs possess a unique anatomical feature of direct connections from the lateral geniculate nucleus (LGN) up to the cortex, which does not exist for other columnar ensembles. In vivo mapping of ODCs has been achieved by several groups using conventional GE-BOLD fMRI contrast (Cheng et al. 2001; Dechent and Frahm 2000; Menon et al. 1997; Yacoub et al. 2007).

In order to *better* resolve submillimeter cortical structures, high spatial resolutions combined with high spatial specificity of the mapping signals are needed. Building on the accomplishments of a long series of theoretical and experimental studies on the underlying mechanisms of fMRI contrast, combined with extensive validation using animal models (e.g., Harel et al. 2006), more recent applications of columnar mapping in humans have been done resulting in more robust ODC maps as well as the first demonstration of orientation columns in the human (Yacoub et al. 2007, 2008).

Limits of Columnar Mapping with fMRI in Humans

Utilizing the advantages of high-field, ODC mapping in humans has been achieved using both GE as well as SE BOLD contrast, with higher specificity of the latter to the underlying neuronal architecture. As was previously shown by anatomical and fMRI studies, ODCs were found to be about ~1 mm in width organized in a periodic layout in primary visual cortex (Fig. 26.1). However, the BOLD contrast sampled not with conventional GE, but probed through SE at ultrahigh magnetic fields (7 T), yielded more accurate ODC maps that were unaffected by nonspecific surface large surface vessels, which normally degrade the accuracy of GE-BOLD maps. In addition, while the overall stimulus invoked changes in fMRI signal intensity were larger for GE-BOLD, column specific differential mapping signals had a *larger* CNR for SE-BOLD at 7 T (Yacoub et al. 2007). The unique anatomical connectivity that provides the ability to visualize ODCs with postmortem staining techniques, granting a priori knowledge of their existence and organization in humans, does *not* exist for other known columnar ensembles. Further, there is no obvious clinical symptom that would reveal the presence, or lack, of such neuronal organization. Therefore, the ability to probe the existence of columnar systems in human requires a highly sensitive, noninvasive, in vivo technique. The potential for high-resolution human fMRI to resolve columnar structures that have not been shown by other methodologies, anatomical or otherwise, would open the doors to neuroscience applications which were previously not possible.

After years of invasive animal studies, *orientation* columns in visual cortex are perhaps the best-known example of such columnar organizations in the brain (e.g., Blasdel 1992; Bonhoeffer and Grinvald 1991; Hubel and Wiesel 1963, 1974). A recent study employed high-field fMRI using SE-based BOLD contrast to investi-

gate the organization for orientation preference in primary visual cortex, a columnar architecture that has been shown to exist in animal models but has *never* been mapped in the human. As a reference, subjects that initially participated in ODC studies (Yacoub et al. 2007) were brought back to map orientation specific regions using the same anatomical slice. Striking similarities were found with the known spatial features and spatial relationships between ODC and orientation columns, as was previously described in monkeys and cat studies using the optical imaging method (Bartfeld and Grinvald 1992; Blasdel 1992; Hubener et al. 1997; Shoham et al. 1997) (Fig. 26.3). These results illustrate the potential of fMRI to investigate unknown submillimeter functional architectures in humans, paving the way for explorations of even more unknown fundamental computational units.

fMRI Mapping of Cortical Lamina

In addition to columnar organizations, neuronal interactions and computational processes are distributed across the cortical lamina, within a cortical column. In cerebral cortex, the laminar distribution of neurons gives rise to six anatomically and functionally distinct layers, numbered sequentially from the surface to the white matter. Each layer receives input from, and projects to, distinct locations. For example, in primary visual cortex, layer IV is the main input layer from the thalamic nuclei; upper layers project mainly forward to higher-order visual areas, while deeper layers project mainly backwards to subcortical structures.

Studies examining changes in fMRI activation as a function of laminar depth, in both humans (Koopmans et al. 2010; Ress et al. 2007) and animal models (Goense and Logothetis 2006; Harel et al. 2006; Silva and Koretsky 2002; Zhao et al. 2006), have detected either faster onset or largest BOLD amplitude changes in the mid-

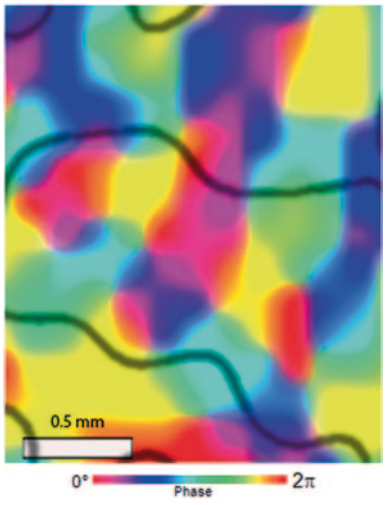

Fig. 26.3 Color represents orientation preference determined by the temporal phase of fMRI signal changes at the stimulus frequency. *Solid black lines* indicate the ODC borders. The scale bar is 0.5 mm. (Taken from Fig. 3 in Yacoub et al. (2008))

dle cortical layers. Further, in order to resolve the laminar origin of the fMRI signals at high fields, a high-resolution fMRI study was correlated with postmortem histological-stained slices obtained within the same animal and tissue region. It was found that tissue fMRI signal changes peak over layer IV when excluding the surface vessels region (Harel et al. 2006).

A recent high-resolution fMRI study by Polimeni et al. (2010) in humans explored functional connectivity of cortical areas based on the laminar distribution of the signals. Using a surface-based analysis, they measured the correlations between visual areas V1 and MT. Anatomical connectivity is well characterized between these areas and has a specific cytoarchitectonic laminar pattern. Interestingly, they report of a peak correlation between layer II/II in area V1 and layer IV in area MT, which corresponds to the output of V1 and the input to MT along the feedforward pathway. Thus, the presence of laminar-specific correlations provides evidence for local hemodynamic control consistent with laminar-specific fMRI measurements.

There are two fundamental confounds when using layer-specific fMRI signals for the purposes of understanding neuronal populations. First, the vascular density (and therefore perfusion and the expected magnitude of the BOLD signal modulation) varies through the cortical depth (Duvernoy et al. 1981). This is particularly true of primary visual cortex, where the extraordinarily high synaptic density in neural layer IV is matched by a high capillary density in the middle of the gray matter thickness (Zheng et al. 1991). A close relationship during development between elaboration of the capillary bed and increasing synaptic density results in an unavoidable confound for fMRI studies (Fonta and Imbert 2002)—vascular density, and therefore BOLD reactivity, tends to be strongest at cortical depths with high synaptic density. Second, there is the effect of the surface vessels which are known to dominate fMRI signals including fMRI based laminar profiles. When high-resolution fMRI is applied the contamination becomes more evident and detrimental to mapping of neuronal architectures even when using a differential paradigm (as opposed to stimulus vs. no stimulus), as demonstrated by recent work on mapping of cortical columns using fMRI (see Fig. 26.1; Yacoub et al. 2007). The recent papers discussing layer-specific fMRI, all used a stimulus versus no stimulus paradigm and all have acknowledged the problem of using the hemodynamic based fMRI signal to infer neuronal activity on this scale.

Recently, Olman and colleagues (Yacoub et al. 2009) reported the first successful differentiation of layer-specific activations in human primary visual cortex. In this work, they demonstrated that there is an observable change in the laminar profile of the V1 fMRI response when subjects view recognizable versus unrecognizable objects. This finding provides direct evidence of the sensitivity of fMRI techniques to neuronal processes in different cortical layers. Neuroscience experiments could benefit enormously from the knowledge of neural computations that can be garnered by detecting and mapping signal changes at different depths in the gray matter, which correspond to different aspects of input, local computation, and output for a given cortical area. Further, thus far, such mapping of neuronal interactions has not been demonstrated in animals or in humans via any neuroimaging methodology.

Future Applications of High-Resolution fMRI

While the described studies represent a significant achievement and a substantial leap in human fMRI studies, due to technical limitations, high-resolution submillimeter fMRI studies of underlying functional architectures were acquired with limited FOVs and the functional maps were only a 2D representation of a complex 3D brain structure. Further, as described above, there are numerous experimental confounds with acquiring such limited volumes. To overcome this, new and more efficient pulse sequences are being developed, allowing for more efficient mapping of these functional domains over larger volumes and in 3D space, while maintaining submillimeter resolutions (Feinberg et al. 2008) (see Fig. 26.2). In addition, capitalizing on the advances of gradient hardware, PI methodology and RF technology, highly accelerated acquisitions (up to 16-fold) (Moeller et al. 2010) will allow for high-resolution imaging of the whole brain on the order of 1 s without much loss in image quality. These new developments will expand the utility of high-field and high-resolution fMRI, allowing the possibility of investigating and probing cortical organizations and dynamics over large volumes at unprecedented spatial and temporal resolutions, which is currently not achievable via any other technique.

References

Bandettini PA, Wong EC, Hinks RS, Tikofsky RS, Hyde JS (1992) Time course EPI of human brain function during task activation. Magn Reson Med 25:390–398

Bartfeld E, Grinvald A (1992) Relationships between orientation-preference pinwheels, cytochrome oxidase blobs, and ocular-dominance columns in primate striate cortex. Proc Natl Acad Sci U S A 89:11905–11909

Blasdel GG (1992) Differential imaging of ocular dominance and orientation selectivity in monkey striate cortex. J Neurosci 12:3115–3138

Blasdel GG, Salama G (1986) Voltage-sensitive dyes reveal a modular organization in monkey striate cortex. Nature 321:579–585

Bonhoeffer T, Grinvald A (1991) Iso-orientation domains in cat visual cortex are arranged in pinwheel-like patterns. Nature 353:429–431

Boxerman JL, Bandettini PA, Kwong KK, Baker JR, Davis TJ, Rosen BR, Weisskoff RM (1995) The Intravascular contribution to fMRI signal changes: Monte Carlo modeling and diffusion-weighted studies in vivo. Magn Reson Med 34:4–10

Chaimow D, Yacoub E, Uğurbil K, Shmuel A (2011) Modeling and analyzing mechanisms underlying fMRI-based decoding of information conveyed in cortical columns. Neuroimage 56(2):627–642

Chaimow D, Yacoub E, Uğurbil K, Shmuel A (2015) Spatial specificity of the functional MRI blood oxygenation response relative to metabolic activity. Annual meting of the Society for Neuroscience, Chicago, USA

Cheng K, Waggoner RA, Tanaka K (2001) Human ocular dominance columns as revealed by high-field functional magnetic resonance imaging. Neuron 32:359–374

de Zwart JA, van Gelderen P, Kellman P, Duyn JH (2002) Application of sensitivity-encoded echo-planar imaging for blood oxygen level-dependent functional brain imaging. Magn Reson Med 48:1011–1020

Dechent P, Frahm J (2000) Direct mapping of ocular dominance columns in human primary visual cortex. Neuroreport 11:3247–3249

Duong TQ, Yacoub E, Adriany G, Hu X, Uğurbil K, Vaughan JT, Merkle H, Kim SG (2002) High-resolution, spin-echo BOLD, and CBF fMRI at 4 and 7 T. Magn Reson Med 48:589–593
Duong TQ, Yacoub E, Adriany G, Hu X, Uğurbil K, Kim SG (2003) Microvascular BOLD contribution at 4 and 7 T in the human brain: gradient-echo and spin-echo fMRI with suppression of blood effects. Magn Reson Med 49:1019–1027
Duvernoy HM, Delon S, Vannson JL (1981) Cortical blood vessels of the human brain. Brain Res Bull 7:519–579
Duyn JH, Moonen CTW, Yperen GH, Boer RW, Luyten PR (1994) Inflow versus deoxyhemoglobin effects in BOLD functional MRI using gradient echoes at 1.5T. NMR Biomed 7:83–88
Engel SA, Rumelhart DE, Wandell BA, Lee AT, Glover GH, Chichilnisky EJ, Shadlen MN (1994) fMRI of human visual cortex. Nature 369:525
Engel SA, Glover GH, Wandell BA (1997) Retinotopic organization in human visual cortex and the spatial precision of functional MRI. Cereb Cortex 7:181–192
Feinberg DA, Oshio K (1991) GRASE (gradient- and spin-echo) MR imaging: a new fast clinical imaging technique. Radiology 181:597–602
Feinberg D, Hoenninger J, Crooks L, Kaufman L, Watts J, Arakawa M (1985) Inner volume MR imaging: technical concepts and their application. Radiology 156:743–747
Feinberg DA, Harel N, Ramanna S, Uğurbil K, Yacoub E (2008) Sub-millimeter single-shot 3D GRASE with inner volume selection for T2-weighted fMRI applications at 7 Tesla. 16th annual meeting of the International Society for Magnetic Resonance in Medicine, Toronto
Fonta C, Imbert M (2002) Vascularization in the primate visual cortex during development. Cereb Cortex 12:199–211
Frahm J, Bruhn H, Merboldt KD (1992) Dynamic MRI of human brain oxygenation during rest and photic stimulation. J Magn Reson Imaging 2:501–505
Frahm J, Merboldt KD, Henicke W (1993) Functional MRI of human brain activation at high spatial resolution. Magn Reson Med 29:139–144
Frahm J, Merboldt KD, Hanicke W, Kleinschmidt A, Boecker H (1994) Brain or vein-oxygenation or flow? On signal physiology in functional MRI of human brain activation. NMR Biomed 7:45–53
Gati JS, Menon RS, Uğurbil K, Rutt BK (1997) Experimental determination of the BOLD field strength dependence in vessels and tissue. Magn Reson Med 38:296–302
Glover GH (1997) Basic and advanced concepts of spiral imaging. ISMRM Fast Workshop Syllabus, Asilomar, CA, pp 115–119
Goense JB, Logothetis NK (2006) Laminar specificity in monkey V1 using high-resolution SE-fMRI. Magn Reson Imaging 24:381–392
Golay X, Pruessmann KP, Weiger M, Crelier GR, Folkers PJ, Kollias SS, Boesiger P (2000) PRESTO-SENSE: an ultrafast whole-brain fMRI technique. Magn Reson Med 43:779–786
Haase A, Frahm J, Matthaei D, Hanicke W, Merboldt, K.-D. (1986) FLASH imaging: rapid NMR imaging using low flip angle pulses. J Magn Reson 67:258–266
Harel N, Lin J, Moeller S, Uğurbil K, Yacoub E (2006) Combined imaging-histological study of cortical laminar specificity of fMRI signals. Neuroimage 29:879–887
Haushofer J, Livingstone MS, Kanwisher N (2008) Multivariate patterns in object-selective cortex dissociate perceptual and physical shape similarity. PLoS Biol 6:e187
Haxby JV, Gobbini MI, Furey ML, Ishai A, Schouten JL, Pietrini P (2001) Distributed and overlapping representations of faces and objects in ventral temporal cortex. Science 293:2425–2430
Haynes JD, Rees G (2005) Predicting the orientation of invisible stimuli from activity in human primary visual cortex. Nat Neurosci 8:686–691
Horton J, Hedley-Whyte ET (1984) Mapping of cytochrome oxidase patches and ocular dominance columns in human visual cortex. Philos Trans R Soc Lond Biol B 304:255–272
Hu X, Kim, S.-G. (1994) Reduction of physiological noise in functional MRI using navigator echo. Magn Reson Med 31:495–503
Hu X, Le TH, Parrish T, Erhard P (1995) Retrospective estimation and correction of physiological fluctuation in functional MRI. Magn Reson Med 34:201–212
Hubel DH, Wiesel TN (1962) Receptive fields, binocular interaction and functional architecture in the cat's visual cortex. J Physiol 160:106–154

Hubel DH, Wiesel TN (1963) Shape and arrangement of columns in cat's striate cortex. J Physiol (Lond) 165:559–568
Hubel DH, Wiesel TN (1974) Sequence regularity and geometry of orientation columns in the monkey striate cortex. J Comp Neurol 158:267–293
Hubel DH, Wiesel TN (1977) Functional architecture of macaque monkey visual cortex. Proc R Soc Lond Biol 198:1–59
Hubener M, Shoham D, Grinvald A, Bonhoeffer T (1997) Spatial relationships among three columnar systems in cat area 17. J Neurosci 17:9270–9284
Hyde JS, Biswal B, Jesmanowicz A (2001) High-resolution fMRI using multislice partial k-space GR-EPI with cubic voxels. Magn Reson Med 46:114–125
Issa NP, Trepel C, Stryker MP (2000) Spatial frequency maps in cat visual cortex. J Neurosci 20:8504–8514
Kalatsky VA, Stryker MP (2003) New paradigm for optical imaging: temporally encoded maps of intrinsic signal. Neuron 38:529–545
Kamitani Y, Tong F (2005) Decoding the visual and subjective contents of the human brain. Nat Neurosci 8:679–685
Klarhofer M, Dilharreguy B, van Gelderen P, Moonen CT (2003) A PRESTO-SENSE sequence with alternating partial-Fourier encoding for rapid susceptibility-weighted 3D MRI time series. Magn Reson Med 50:830–838
Koopmans PJ, Barth M, Norris DG (2010) Layer-specific BOLD activation in human V1. Hum Brain Mapp 31:1297–1304
Kruger G, Glover GH (2001) Physiological noise in oxygenation-sensitive magnetic resonance imaging. Magn Reson Med 46:631–637
Kwong KK, Belliveau JW, Chesler DA, Goldberg IE, Weisskoff RM, Poncelet BP, Kennedy DN, Hoppel BE, Cohen MS, Turner R, Cheng H-M, Brady TJ, Rosen BR (1992) Dynamic magnetic resonance imaging of human brain activity during primary sensory stimulation. Proc Natl Acad Sci U S A 89:5675–5679
Lai S, Hopkins AL, Haacke EM, Li D, Wasserman BA, Buckley P, Friedman L, Meltzer H, Hedera P, Friedland R (1993) Identification of vascular structures as a major source of signal contrast in high resolution 2D and 3D functional activation imaging of the motor cortex at 1.5 T: preliminary results. Magn Reson Med 30:387–392
Larkman DJ, Hajnal JV, Herlihy AH, Coutts GA, Young IR, Ehnholm G (2001) Use of multicoil arrays for separation of signal from multiple slices simultaneously excited. J Magn Reson Imaging 13:313–317
Lee AT, Glover GH, Meyer GH (1995) Discrimination of large venous vessels in time-course spiral blood-oxygen-level-dependent magnetic resonance functional neuroimaging. Magn Reson Med 33:745–754
Liu G, Sobering G, Duyn J, Moonen CT (1993) A functional MRI technique combining principles of echo-shifting with a train of observations (PRESTO). Magn Reson Med 30:764–768
Mansfield P (1977) Multi-planar image formation using NMR spin echoes. J Phys C: Solid State Phys 10:L55–L58
Mansfield P, Harvey PR, Stehling MK (1994) Echo-volumar imaging. MAGMA 2:291–294
Menon R, Ogawa S, Strupp JP, Uğurbil K (1997) Ocular dominance in human V1 demonstrated by functional magnetic resonance imaging. J Neurophysiol 77:2780–2787
Meyer CH, Hu BS, Nishimura DG, Macovski A (1992) Fast spiral coronary artery imaging. Magn Reson Med 28:202–213
Miller KL, Jezzard P (2008) Modeling SSFP functional MRI contrast in the brain. Magn Reson Med 60:661–673
Moeller S, Yacoub E, Auerbach E, van de Moortele PF, Adriany G, Uğurbil K (2008) fMRI with 16 fold reduction using multibanded multislice sampling. Proc Int Soc for Mag Reson Med, Toronto
Moeller S, Van de Moortele PF, Goerke U, Adriany G, Uğurbil K (2006) Application of parallel imaging to fMRI at 7 Tesla utilizing a high 1D reduction factor. Magn Reson Med 56:118–129

Moeller S, Yacoub E, Olman CA, Auerbach E, Strupp J, Harel N, Uğurbil K (2010) Multiband multislice GE-EPI at 7 T, with 16-fold acceleration using partial parallel imaging with application to high spatial and temporal whole-brain fMRI. Magn Reson Med 63:1144–1153

Moon CH, Fukuda M, Park SH, Kim SG (2007) Neural interpretation of blood oxygenation level-dependent fMRI maps at submillimeter columnar resolution. J Neurosci 27:6892–6902

Mountcastle VB (1957) Modality and topographic properties of single neurons of cat's somatic sensory cortex. J Neurophysiol 20:408–434

Neggers SF, Hermans EJ, Ramsey NF (2008) Enhanced sensitivity with fast three-dimensional blood-oxygen-level-dependent functional MRI: comparison of SENSE-PRESTO and 2D-EPI at 3 T. NMR Biomed 21:663–676

Noll D, Cohen J, Meyer C, Schneider W (1995) Spiral K-space MR imaging of cortical activation. J Magn Reson Imaging 5:49–57

Ogawa S, Lee T-M, Kay AR, Tank DW (1990) Brain magnetic resonance imaging with contrast dependent on blood oxygenation. Proc Natl Acad Sci U S A 87:9868–9872

Ogawa S, Tank DW, Menon R, Ellermann JM, Kim S-G, Merkle H, Uğurbil K (1992) Intrinsic signal changes accompanying sensory stimulation: functional brain mapping with magnetic resonance imaging. Proc Natl Acad Sci U S A 89:5951–5955

Ogawa S, Lee TM, Barrere B (1993) Sensitivity of magnetic resonance image signals of a rat brain to changes in the cerebral venous blood oxygenation. Magn Reson Med 29:205–210

Olman CA, Van de Moortele PF, Schumacher JF, Guy JR, Uğurbil K, Yacoub E (2010) Retinotopic mapping with spin echo BOLD at 7T. Magn Reson Imaging. 28:1258–1569

Parkes LM, Schwarzbach JV, Bouts AA, Deckers RH, Pullens P, Kerskens CM, Norris DG (2005) Quantifying the spatial resolution of the gradient echo and spin echo BOLD response at 3 Tesla. Magn Reson Med 54:1465–1472

Pfeuffer J, Van De Moortele PF, Yacoub E, Adriany G, Andersen P, Merkle H, Garwood M, Uğurbil K, Hu X (2002) Zoomed functional imaging in the human brain at 7 Tesla with simultaneously high spatial and temporal resolution. Neuroimage 17:272–286

Polimeni JR, Fischl B, Greve DN, Wald LL (2010) Laminar analysis of 7T BOLD using an imposed spatial activation pattern in human V1. Neuroimage 52:1334–1346

Poser BA, Norris DG (2007) Fast spin echo sequences for BOLD functional MRI. MAGMA 20:11–17

Poser BA, Koopmans PJ, Witzel T, Wald LL, Barth M (2010) Three dimensional echo-planar imaging at 7 Tesla. Neuroimage 51:261–266

Pruessmann KP, Weiger M, Scheidegger MB, Boesiger P (1999) SENSE: sensitivity encoding for fast MRI. Magn Reson Med 42:952–962

Ress D, Glover GH, Liu J, Wandell BA (2007) Laminar profiles of functional activity in the human brain. Neuroimage 34:74–84

Schafer A, van der Zwaag W, Francis ST, Head KE, Gowland PA, Bowtell RW (2007) High resolution SE-fMRI in humans at 3 and 7 T using a motor task. MAGMA. 21:113–120

Shmuel A, Grinvald A (1996) Functional organization for direction of motion and its relationship to orientation maps in cat area 18. J Neurosci 16:6945–6964

Shmuel A, Yacoub E, Chaimow D, Logothetis NK, Uğurbil K (2007) Spatio-temporal point-spread function of fMRI signal in human gray matter at 7 Tesla. Neuroimage 35:539–552

Shmuel A, Chaimow D, Raddatz G, Uğurbil K, Yacoub E (2010) Mechanisms underlying decoding at 7 T: ocular dominance columns, broad structures, and macroscopic blood vessels in V1 convey information on the stimulated eye. Neuroimage 49:1957–1964

Shoham D, Hubener M, Schulze S, Grinvald A, Bonhoeffer T (1997) Spatio-temporal frequency domains and their relation to cytochrome oxidase staining in cat visual cortex. Nature 385:529–533

Silva AC, Koretsky AP (2002) Laminar specificity of functional MRI onset times during somatosensory stimulation in rat. Proc Natl Acad Sci U S A 99:15182–15187

Silva AC, Barbier EL, Lowe IJ, Koretsky AP (1998) Radial echo-planar imaging. J Magn Reson 135:242–247

Sodickson DK, Griswold MA, Jakob PM (1999) SMASH imaging. Magn Reson Imag Clin N Am 7:237–254, vii–viii

Swisher JD, Gatenby JC, Gore JC, Wolfe BA, Moon CH, Kim SG, Tong F (2010) Multiscale pattern analysis of orientation-selective activity in the primary visual cortex. J Neurosci 30:325–330

Triantafyllou C, Hoge RD, Krueger G, Wiggins CJ, Potthast A, Wiggins GC, Wald LL (2005) Comparison of physiological noise at 1.5 T, 3 T and 7 T and optimization of fMRI acquisition parameters. Neuroimage 26:243–250

Ts'o DY, Frostig RD, Lieke EE, Grinvald A (1990) Functional organization of primate visual cortex revealed by high resolution optical imaging. Science 249:417–420

Uğurbil K (2012) The road to functional imaging and ultrahigh fields. Neuroimage 62:726–735

Uğurbil K (2014) Magnetic resonance imaging at ultrahigh fields. IEEE Trans Biomed Eng 61:1364–1379

Uğurbil K, Adriany G, Andersen P, Chen W, Garwood M, Gruetter R, Henry PG, Kim SG, Lieu H, Tkac I, Vaughan T, Van De Moortele PF, Yacoub E, Zhu XH (2003) Ultrahigh field magnetic resonance imaging and spectroscopy. Magn Reson Imaging 21:1263–1281

Uğurbil K, Muller-Bierl B, Uğurbil K (2009) An integrative model for neuronal activity-induced signal changes for gradient and spin echo functional imaging. Neuroimage 48:150–165

Van de Moortele PF, Auerbach EJ, Olman C, Yacoub E, Uğurbil K, Moeller S (2009) T1 weighted brain images at 7 Tesla unbiased for Proton Density, T_2^* contrast and RF coil receive B1 sensitivity with simultaneous vessel visualization. Neuroimage 46:432–446

Vaughan JT, Garwood M, Collins CM, Liu W, DelaBarre L, Adriany G, Andersen P, Merkle H, Goebel R, Smith MB, Uğurbil K (2001) 7T vs. 4T: RF power, homogeneity, and signal-to-noise comparison in head images. Magn Reson Med 46:24–30

Weliky M, Bosking WH, Fitzpatrick D (1996) A systematic map of direction preference in primary visual cortex. Nature 379:725–728

Yacoub E, Shmuel A, Pfeuffer J, Van De Moortele PF, Adriany G, Andersen P, Vaughan JT, Merkle H, Uğurbil K, Hu X (2001) Imaging brain function in humans at 7 Tesla. Magn Reson Med 45:588–594

Yacoub E, Duong TQ, Van De Moortele PF, Lindquist M, Adriany G, Kim SG, Uğurbil K, Hu X (2003) Spin-echo fMRI in humans using high spatial resolutions and high magnetic fields. Magn Reson Med 49:655–664

Yacoub E, Shmuel A, Logothetis N, Uğurbil K (2007) Robust detection of ocular dominance columns in humans using Hahn Spin Echo BOLD functional MRI at 7 Tesla. Neuroimage 37:1161–1177

Yacoub E, Harel N, Uğurbil K (2008) High-field fMRI unveils orientation columns in humans. Proc Natl Acad Sci U S A 105:10607–10612

Yacoub E, Uğurbil K, Olman C (2009) Feasibility of detecting differential layer specific activations in humans using SE BOLD FMRI at 7 T. Proc Mag Reson Med, Honolulu

Yang Y, Glover GH, van Gelderen P, Mattay VS, Santha AK, Sexton RH, Ramsey NF, Moonen CT, Weinberger DR, Frank JA, Duyn JH (1996) Fast 3D functional magnetic resonance imaging at 1.5 T with spiral acquisition. Magn Reson Med 36:620–626

Yang Y, Mattay V, Weinberger D, Frank J (1997) Localized Echo-volume Imaging- Methods for functional MRI. J Magn Reson Imaging 7:371–375

Ye Y, Zhuo Y, Xue R, Zhou XJ (2010) BOLD fMRI using a modified HASTE sequence. Neuroimage 49:457–466

Zhao F, Wang P, Hendrich K, Uğurbil K, Kim SG (2006) Cortical layer-dependent BOLD and CBV responses measured by spin-echo and gradient-echo fMRI: insights into hemodynamic regulation. Neuroimage 30:1149–1160

Zheng D, LaMantia AS, Purves D (1991) Specialized vascularization of the primate visual cortex. J Neurosci 11:2622–2629